Discrete Spatial Compression Beyond Beamspace Channel Sparsity Based on Branch-and-Bound

Zhiyuan Jiang, Sheng Zhou, and Zhisheng Niu, *Fellow, IEEE*
TNList, Tsinghua University, {zhiyuan,sheng.zhou,niuzhs}@tsinghua.edu.cn

***Abstract*—One of the most challenging issues in deploying massive multiple-input multiple-output (MIMO) systems is the significant radio-frequency (RF) front-end complexity, hardware cost and power consumption. Towards this end, the beamspace-MIMO based approach is a promising solution. In this paper, we first show that traditional beamspace-MIMO approaches suffer from spatial power leakage and imperfect channel statistics estimation. A beam combination module is hence proposed, which consists of a small number (compared with the number of antenna elements) of low-resolution (possibly one-bit) digital (discrete) phase shifters after beamspace transformation to further compress the beamspace signal dimensionality, such that the number of RF chains can be reduced beyond beamspace transformation and beam selection. The optimum discrete beam combination weights are obtained based on the branch-and-bound (BB) approach. The key to the BB-based solution is to solve the embodied sub-problem, whose solution is derived in a closed-form. Link-level simulation results based on realistic channel models and LTE parameters are presented which show that the proposed schemes can reduce the number of RF chains by up to 25% with a one-bit phase-shifter-network.**

I. Introduction

Massive multiple-input multiple-output (MIMO) systems will play a pivotal role in the next generation cellular systems. Deploying a large number of base station (BS) antenna brings tremendous spatial degree-of-freedoms (DoFs), which can significantly improve the system performance. Despite the potential benefits, the practical implementation of massive MIMO systems faces critical challenges. One of them is the related cost, including hardware cost and power consumption of radio frequency (RF) chains [1]. In view of these, the hybrid beamforming architecture has been proposed [2]–[4], which adopts an RF analog beamforming module to create beam-based signals, which are usually with lower dimensionality compared with antenna-based ones due to spatial signal concentration. The RF chains are connected to beams instead of antennas such that the quantity is significantly reduced. In this respect, the lens antenna array, or beamspace MIMO architecture [5], by which the lens antenna array is adopted as the analog beamforming module is one promising solution. The lens antenna array transforms the signal to angular domain by a lens-like equipment. See Fig. 1 for an instance. Such an approach is shown to be very effective which can reduce the number of RF chains dramatically with little performance degradation [6].

In this paper, in addition to the beamspace massive MIMO transformation, we aim to further reduce the number of RF chains dramatically by beam combination with a low-resolution phase shifter network (PSN). The beam combination module tracks the signal subspace by dimensionality-reduced beamforming. The architecture is described in Fig. 1. Since the RF beamforming module should be simplified with low-cost hardware to enable widely usage in, e.g., remote-radio-units (RRUs) in cloud radio access networks (C-RAN) systems, the beam combination module is composed of low-resolution (B bits which equals 2^B phase shifting states) digital phase shifters with constant amplitudes. The main contribution is that a branch-and-bound (BB) method is proposed to obtain the optimum beamforming weights with constant amplitudes and limited-resolution (possibly one-bit) digital phase shifters. The most prominent contribution is that we solve the sub-problem in the BB method in a closed-form. We conduct realistic link-level simulations with canonical 3GPP spatial channel models to validate our proposed schemes. The proofs of the main results are omitted in this paper due to lack of space. Interested readers can refer to [7].

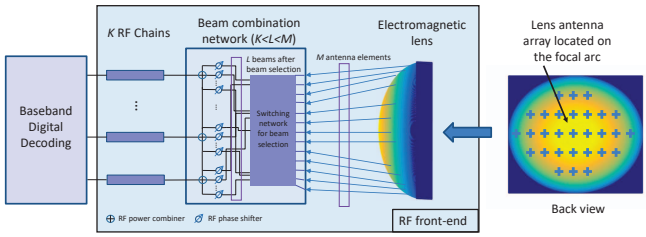

Fig. 1. Proposed beamspace massive MIMO system overview. The phase shifter network is used for beam combination to further reduce the RF complexity, consisting of finite-resolution digital phase shifters.

II. System Model and Preliminaries

A. Signal Model

We consider the uplink (UL) of a single cell system. The UL baseband equivalent signal model is written as $\boldsymbol{y} = \boldsymbol{H}\boldsymbol{x} + \boldsymbol{n}$, where the UL receive signal, i.e., $\boldsymbol{y}$, is a complex vector of dimension M, and M is the total number of antenna elements. Vector $\boldsymbol{x}$ is the uplink transmit signals from N users. The identically-independently distributed (i.i.d.) Gaussian additive noise is denoted by $\boldsymbol{n}$. Denote by $\boldsymbol{h}_{n,i}$ as the channel vector from the i-th antenna of user n to M receive antennas. Each user is equipped with A_n antennas, and together they form $\boldsymbol{x}$ of dimension $A = \sum_{n=1}^{N} A_n$. Denote by $\boldsymbol{H}$ is the channel matrix of dimension $M \times A$. Without loss of generality, the narrowband signal model is adopted whereby the signal

978-1-5386-3180-5/18/$31.00 ©2018 IEEE

bandwidth is much smaller than the carrier frequency. Denote the signal after receive beamforming as

$$\boldsymbol{c} = \boldsymbol{D}\boldsymbol{A}_{\mathcal{C}}\boldsymbol{A}_{\mathcal{L}}\boldsymbol{y}, \tag{1}$$

where the RF beamforming (beamspace transformation) at the lens antenna array and the beam selection are denoted by $\boldsymbol{A}_{\mathcal{L}} \in \mathbb{C}^{L\times M}$ (L beams are selected), the beam combination proposed by this paper is denoted by $\boldsymbol{A}_{\mathcal{C}} \in \mathbb{C}^{K\times L}$, and the baseband digital receive beamforming is denoted by $\boldsymbol{D} \in \mathbb{C}^{A\times K}$ and hence K is the number of RF chains. In this paper, the beam combination is subject to hardware constraints to reduce the RF hardware complexity. Therefore, the beam combination matrix is restricted to have unit-amplitude entries and limited phase-resolution, i.e.,

$$[\boldsymbol{A}_{\mathcal{C}}]_{i,j} \in \boldsymbol{\Psi},\ \boldsymbol{\Psi} = \left\{ e^{\frac{j2n\pi}{2^B}},\ n = 0, ..., 2^B - 1. \right\}, \tag{2}$$

where B is the resolution of the digital phase shifters, and $B = 1$ denotes the one-bit PSN where there are only two states of the phase shifters, i.e., $[\boldsymbol{A}_{\mathcal{C}}]_{i,j} \in \{-1, 1\}$.

B. Channel Model

Using a geometry-based channel model [8], the channel vector can be written as

$$\boldsymbol{h}_{n,i} = \sqrt{\frac{M}{R_{n,i}}} \sum_{r=1}^{R_{n,i}} \beta_{n,r}\boldsymbol{\alpha}(\theta_{n,r}, \psi_{n,r}), \tag{3}$$

where $R_{n,i}$ denotes the total number of multi-path components (MPCs) in the propagation channel for the i-th antenna of user n, the amplitude of each MPC is denoted by $\beta_{n,r}$, and $\mathbb{E}[|\beta_{n,r}|^2] = \gamma_{n,r}$. The azimuth and elevation angle-of-arrival (AoA) of the r-th arriving MPC of user n are denoted by $\theta_{n,r}$ and $\psi_{n,r}$, respectively. The steering vector for one MPC (assuming uniform linear array) is $\boldsymbol{\alpha}(\theta_{n,r}) = \frac{1}{\sqrt{M}} \left[e^{-j2\pi m \frac{d\sin\theta_{n,r}}{\lambda}} \right]$, $m \in \left\{ s - \frac{M-1}{2}, s = 0, 1, ..., M-1 \right\}$, where d is the antenna spacing[1] and λ is the wavelength. Summing up all the contributing MPCs obtains the compound channel representation in (3). For a judiciously designed lens antenna array, the beamspace transformation is equivalent to a DFT where each column of the DFT matrix is the uniform linear array signal from a specific AoA [9], i.e., assuming without beam selection, $\boldsymbol{A}_{\mathcal{L}} = [\boldsymbol{\alpha}(\theta_1), \boldsymbol{\alpha}(\theta_2), ..., \boldsymbol{\alpha}(\theta_M)]^{\dagger}$, $\sin\theta_i = \frac{\lambda}{dM}\left(i - \frac{M+1}{2}\right)$. For a two-dimension lens antenna array, it can be derived that $\boldsymbol{A}_{\mathcal{L},\text{2D}} = \boldsymbol{A}_{\mathcal{L},\text{row}} \otimes \boldsymbol{A}_{\mathcal{L},\text{col}}$. The channel correlation matrix (CCM) of $\boldsymbol{h}_{n,i}$ is defined as

$$\boldsymbol{R}_{n,i} = \mathbb{E}\left[\boldsymbol{h}_{n,i}\boldsymbol{h}_{n,i}^{\dagger} \right]. \tag{4}$$

Denote the SVD of the CCM as $\boldsymbol{R}_{n,i} = \boldsymbol{U}_{n,i}\boldsymbol{\Sigma}_{n,i}\boldsymbol{U}_{n,i}^{\dagger}$, where we always assume the singular values are arranged in non-increasing order. Based on (4) wherein the expectation is taken over MPC channel gain $\beta_{n,r}$, it follows that

$$\boldsymbol{R}_{n,i} = \frac{M}{R_{n,i}} \sum_{r=1}^{R_{n,i}} \gamma_{n,r}\boldsymbol{\alpha}(\theta_{n,r}, \psi_{n,r})\boldsymbol{\alpha}(\theta_{n,r}, \psi_{n,r})^{\dagger}. \tag{5}$$

[1]We assume the so-called critical antenna spacing, i.e., $d = \lambda/2$.

It is observed that the CCM is the summation of all the rank-1 matrices constructed by the steering vectors of MPCs. The cross terms of the steering vectors are averaged out because different MPCs usually have independently distributed small scale fading amplitude coefficients [10]. It is straightforward to derive that

$$\begin{aligned}\boldsymbol{R}_{\text{t}} = \mathbb{E}\left[\boldsymbol{H}\boldsymbol{H}^{\dagger}\right] = \mathbb{E}\left[\sum_{n,i}\boldsymbol{h}_{n,i}\boldsymbol{h}_{n,i}^{\dagger}\right] = \sum_{n,i}\boldsymbol{R}_{n,i} \\ = \sum_{n,i}\frac{M}{R_{n,i}}\sum_{r=1}^{R_{n,i}}\gamma_{n,r}\boldsymbol{\alpha}(\theta_{n,r}, \psi_{n,r})\boldsymbol{\alpha}(\theta_{n,r}, \psi_{n,r})^{\dagger}. \end{aligned} \tag{6}$$

Alternatively, $\boldsymbol{R}_{\text{t}}$ can be interpreted as the overall CCM which consists of the MPCs from all users. The overall CCM is usually obtained by averaging the receive signal over a number of time and frequency resources, i.e.,

$$\bar{\boldsymbol{R}}_{\text{t}} = \frac{1}{TL}\sum_{t,l}\boldsymbol{y}_{t,l}\boldsymbol{y}_{t,l}^{\dagger}, \tag{7}$$

where the average is over time (indexed by t) and frequency (indexed by l) receive symbols. The method is widely used in practice. More sophisticated CCM estimation algorithm can be found in, e.g., [11]. The time-averaged useful signal CCM is defined as $\bar{\boldsymbol{R}}_{\text{s}} = \frac{1}{TL}\sum_{t,l}\boldsymbol{H}_{t,l}\boldsymbol{x}_{t,l}\boldsymbol{x}_{t,l}^{\dagger}\boldsymbol{H}_{t,l}^{\dagger}$, where it is approximated that $\bar{\boldsymbol{R}}_{\text{s}} \approx \bar{\boldsymbol{R}}_{\text{t}} - \sigma^2\boldsymbol{I}_M$, and σ^2 denotes the noise variance. On one hand, the approximation in here is due to the cross-correlation between channel coefficients. On the other hand, the insufficient time and frequency samples may also affect the approximation since the approximation is met exactly based on ensemble-average but not so with time-average CCM. The spatial compression efficiency, which is defined as the reserved signal power ratio in a given signal block by a limited number of RF chains after spatial compression including beamspace transformation and proposed beam combination, is written as

$$\eta\left(\boldsymbol{A}_{\mathcal{C}}\right) = \frac{\text{tr}\left[\boldsymbol{A}_{\mathcal{C}}\boldsymbol{A}_{\mathcal{L}}\bar{\boldsymbol{R}}_{\text{s}}\boldsymbol{A}_{\mathcal{L}}^{\dagger}\boldsymbol{A}_{\mathcal{C}}^{\dagger}\right]}{\text{tr}\bar{\boldsymbol{R}}_{\text{s}}}, \tag{8}$$

where it is prescribed that $\boldsymbol{A}_{\mathcal{C}}$ has orthonormal rows such that the transform efficiency is well defined with range $\eta \in [0, 1]$. Since the beamspace transformation is considered to be fixed in this paper, the spatial compression efficiency is only a function of beam combination matrix $\boldsymbol{A}_{\mathcal{C}}$.

C. Spatial Compression Procedure

The central goal of the paper is to design $\boldsymbol{A}_{\mathcal{C}}$ subject to the hardware constraints in (2), so as to further reduce the number of RF chains, i.e., K. Towards this end, the general procedure to obtain the combination weights is described below. The detailed algorithm is illustrated later in Section IV.

1) Channel Estimation: First, the CCM after beamspace transformation is obtained by sweeping over all beams. This is achieved by setting the phase shifters to off state or zero phase (corresponding to unity) to realize beam switching. Advanced algorithms which leverage the compressive-sensing technique and avoid a complete beam sweeping can be found in [12].

2) Beam Combination Weights Determination: After the CCM is obtained, the combination weights $\boldsymbol{A}_{\mathcal{C}}$ is determined by the proposed algorithms described in Section IV.

3) Data Transmission: Then, the baseband digital processing is performed over the beam-domain signal after beam combination. The time duration between adjacent beam combination weights design is related to the CCM variation speed (1 second to 10 seconds [13]), which is in general much slower than instantaneous CSI (micro-seconds). Therefore, the channel estimation overhead is relatively low.

III. Why Beamspace Transformation is not Enough for RF Chain Reduction?

The beamspace transformation takes advantages of the angular power sparsity of massive MIMO channels to reduce the number of RF chains by selecting the most significant signal directions [5]. The theoretical support of the approach stems from the fact that the optimal spatial compression scheme is proved to be SVD-based [14], and that the DFT-based beamspace transformation is asymptotically equivalent to SVD approach when the number of antennas is large and the time averaged CCM estimation equals the ensemble-averaged CCM [13]. In what follows, examples are given to demonstrate that when these two conditions are not met exactly in practice, we can further reduce the number of RF chains by combining correlated beams which essentially experience correlated propagation channels.

It is a known fact that the DFT suffers from power leakage, especially when the number of the DFT points is limited. In [9], [15], it is proved that the power leakage P_{leak} of a beam given the AoA θ and beam index is approximated by $P_{\text{leak}} \sim \text{sinc}^2\left(m - \frac{d\sin(\theta)}{\lambda}\right)$, where $\text{sinc}(x) \triangleq \frac{\sin(x)}{x}$ and m is the beam index. Fig. 2 shows that when the AoA coincides with the AoA of some DFT vector, e.g., AoA is zero corresponding to the first DFT vector, then only one beam after the beamspace transformation can perfectly contain all the signal power. In this case, only one RF chain is required with spatial compression efficiency of 1. However, the case with a slightly different AoA wherein $\theta = 0.063$ shows a significant power leakage. In this circumstance, more than one RF chains are needed to achieve a target compression efficiency. Previous work [9], [15] usually assumes the ideal case which ignores this effect by assuming the AoAs are always matched to the DFT vectors. Based on this example, it can be anticipated that there is potential to reduce the number of RF chains beyond beamspace transformation in general propagation environments.

On the other hand, it is likely that the time-averaged CCM in (7) does not converge to the ensemble-average CCM in (6) due to finite time and frequency samples which could also lead to potential RF chain waste. Concretely, suppose a channel vector with 3 MPCs in total. If there is infinite samples, in theory the effective rank (effectively significant rank) of the CCM should be 3 assuming i.i.d. fading for each MPC. However, consider an extreme example where the channel is static in the given signal block, which happens when the user and the scatterers are both static during the time, and consequently the rank of the CCM estimated in the signal block is 1. As a result, one beam is sufficient. In the mean time, there are still 3 different MPCs with distinct AoAs, and hence the beamspace transformation detects 3 beams (ignoring spatial leakage). In this case, 2 RF chains are wasted and they could be saved for less RF complexity.

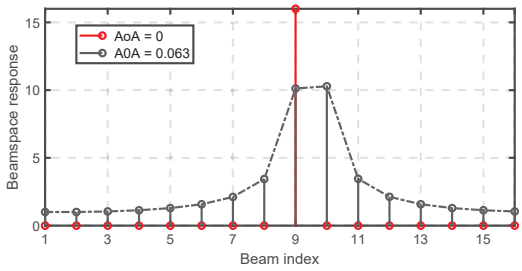

Fig. 2. An MPC angular power spectrum example with 16 antennas.

Based on the insights provided in the above examples, we propose to adopt a beam combination module after the lens antenna array to further reduce the number of required RF chains. Furthermore, hardware constrains are considered where limited-resolution digital phase shifters are adopted.

IV. Beam Combination Schemes with Hardware Constraints

After beam selection by the switching network, the selected beams are combined to further reduce the number of RF chains by a finite-resolution PSN. The problem of maximizing the spatial compression efficiency subject to **hardware constraint** is formulated by

$$\textbf{P1:} \quad \underset{\boldsymbol{A}_{\mathcal{C}}}{\text{maximize}}\ \eta\left(\boldsymbol{A}_{\mathcal{C}}\right) = \frac{\text{tr}\left[\boldsymbol{A}_{\mathcal{C}}\boldsymbol{A}_{\mathcal{L}}\bar{\boldsymbol{R}}_{\text{s}}\boldsymbol{A}_{\mathcal{L}}^{\dagger}\boldsymbol{A}_{\mathcal{C}}^{\dagger}\right]}{\text{tr}\bar{\boldsymbol{R}}_{\text{s}}} \quad \text{s.t.,}\ \left[\boldsymbol{A}_{\mathcal{C}}\right]_{i,j} \in \left\{e^{\frac{j2n\pi}{2^B}},\, n = 0, ..., 2^B - 1\right\}. \tag{9}$$

It is observed that the problem is a combinatorial problem with a large scale, which is generally NP-hard. In this paper, we adopt a BB-based approach to solve for the optimum solution which, admittedly, has a high complexity but with optimality. Therefore, it can be viewed as a performance upper bound for the other low-complexity heuristic algorithms. The BB algorithm is a widely-used method to solve discrete programming problem which is guaranteed to converge to optimum. However, the most critical challenge in developing a BB-based approach is to *solve the sub-problem* in order to find an appropriate bound for each branch, hence the name "branch and bound". Interested readers can see, e.g., [16], for the details about the BB algorithm. Without further complications, the sub-problem is a problem about what are the optimum weights when a subset of the weights is given, which can be formulated as

$$\textbf{P2:} \quad \underset{\boldsymbol{w}_{\text{J}}}{\text{maximize}}\ \eta(\boldsymbol{x}) \triangleq \frac{\boldsymbol{x}^{\dagger}\boldsymbol{R}\boldsymbol{x}}{\boldsymbol{x}^{\dagger}\boldsymbol{x}}, \quad \text{s.t.,}\ \boldsymbol{x} = [\boldsymbol{d}_{\text{I}}^{T},\, \boldsymbol{w}_{\text{J}}^{T}]^{T}, \tag{10}$$

where $\boldsymbol{R}$ is Hermitian positive semi-definite, $\boldsymbol{x} \in \mathbb{C}^L$, $\boldsymbol{d}_{\rm I} \in \mathbb{C}^l$ is a given complexed-valued vector, and $1 \leq l \leq L$. For ease of exposition, denote $\boldsymbol{R} = \begin{bmatrix} \boldsymbol{R}_{\rm I} & \boldsymbol{R}_{\rm IJ} \\ \boldsymbol{R}_{\rm JI} & \boldsymbol{R}_{\rm J} \end{bmatrix}$, where $\boldsymbol{R}_{\rm IJ} = \boldsymbol{R}_{\rm JI}^{\dagger}$. The SVD of $\boldsymbol{R}_{\rm J}$ is $\boldsymbol{R}_{\rm J} = \boldsymbol{U}_{\rm J}\boldsymbol{\Sigma}_{\rm J}\boldsymbol{U}_{\rm J}^{\dagger}$, where $\boldsymbol{\Sigma}_{\rm J} = {\rm diag}[\lambda_1, ..., \lambda_{L-l}]$ and $\lambda_1 \geq \lambda_2 \geq ... \geq \lambda_{L-l}$. Denote $\boldsymbol{u}_{\rm J,dom}$ as one of the dominant singular vector of $\boldsymbol{R}_{\rm J}$, $\boldsymbol{p} \triangleq \boldsymbol{R}_{\rm JI}\boldsymbol{d}_{\rm I}$, $r \triangleq \boldsymbol{d}_{\rm I}^{\dagger}\boldsymbol{R}_{\rm I}\boldsymbol{d}_{\rm I}$, and $d \triangleq \boldsymbol{d}_{\rm I}^{\dagger}\boldsymbol{d}_{\rm I}$. This sub-problem is directly derived from solving **P1** step by step by the BB method, and relax the discrete constraints to continuous to obtain an upper bound. Concretely, the optimization in **P2** is over $\boldsymbol{x}$ which is one column of $\boldsymbol{A}_{\mathcal{C}}$, given $\boldsymbol{R}$ as the CCM after beamspace transformation and beam selection, i.e., $\boldsymbol{R} = \boldsymbol{A}_{\mathcal{L}}\bar{\boldsymbol{R}}_{\rm s}\boldsymbol{A}_{\mathcal{L}}^{\dagger}$. We emphasize that even without the discrete constrains, the sub-problem **P2**, being a non-convex problem since the objective function is not concave, is still very difficult to solve. It is observed through numerical results that the global optimum solution is not attainable by a commonly-used, e.g., gradient-ascend-based method. In the following theorem, we derive the **optimum solution** in a closed-form (given the SVD of $\boldsymbol{R}$) based on a constructive proof, wherein we hypothesis the solution has a special structure and prove that such a structure is indeed the optimum solution.

Theorem 1: The optimum objective value of **P2** is given by

$$\eta^*(\boldsymbol{d}_{\rm I}) = \begin{cases} \max[\lambda_1, r/d], \text{ if } \boldsymbol{u}_{\rm J,dom}^{\dagger}\boldsymbol{p} = 0 \text{ and C1} \\ \lambda^*, \text{ otherwise,} \end{cases} \tag{11}$$

where the condition C1 is

$$\text{C1}: \qquad \lambda_1 d - r - \sum_{i=m+1}^{L-l} \frac{\left|\left(\boldsymbol{U}_{\rm J}^{\dagger}\boldsymbol{p}\right)_i\right|^2}{\lambda_1 - \lambda_i} > 0, \tag{12}$$

and m is the dimensionality of the dominant singular subspace of $\boldsymbol{R}_{\rm J}$, and λ^* satisfies $\lambda_1 < \lambda^* \leq \frac{d\lambda_1 + r + \sqrt{(d\lambda_1 - r)^2 + 4d\boldsymbol{p}^{\dagger}\boldsymbol{p}}}{2d}$, and λ^* is the unique solution of the equation

$$\sum_{i=1}^{L-l} \frac{\left(\boldsymbol{U}_{\rm J}^{\dagger}\boldsymbol{p}\right)_i}{\lambda - \lambda_i} = \lambda d - r. \tag{13}$$

The optimum solution $\boldsymbol{w}_{\rm J}^*$ is

$$\boldsymbol{w}_{\rm J}^* = \begin{cases} \beta\boldsymbol{u}_{\rm J,dom} \text{ or } \boldsymbol{0}, & \text{if } \boldsymbol{u}_{\rm J,dom}^{\dagger}\boldsymbol{p} = 0 \text{ and C1}, \\ \left(\lambda^*\boldsymbol{I}_{L-l} - \boldsymbol{R}_{\rm J}\right)^{-1}\boldsymbol{p}, & \text{otherwise}, \end{cases} \tag{14}$$

where $\beta \to \infty$.

Proof: The proof is omitted due to lack of space. ■

Remark 1: It is noteworthy that the limiting case of Theorem 1, i.e., $\boldsymbol{u}_{\rm J,dom}^{\dagger}\boldsymbol{p} = 0$ and C1, almost never happens in practice since the condition is very strict. Therefore, the case is derived more for mathematical completeness rather than practical concerns.

Corollary 1: An approximation of the optimum solution of **P2** with discrete constraints in (2) is $\eta_{\rm appox}(\boldsymbol{d}_{\rm I}) = \frac{\boldsymbol{d}_{\rm I}^{\dagger}\boldsymbol{R}_{\rm I}\boldsymbol{d}_{\rm I} + (\boldsymbol{w}_{\rm J}^*)^{\dagger}\boldsymbol{R}_{\rm J}\boldsymbol{w}_{\rm J}^* + \boldsymbol{p}^{\dagger}\boldsymbol{w}_{\rm J}^* + (\boldsymbol{w}_{\rm J}^*)^{\dagger}\boldsymbol{p} + \sigma_{\boldsymbol{e}}^2\frac{{\rm tr}\boldsymbol{R}_{\rm J}}{L-l}}{\boldsymbol{d}_{\rm I}^{\dagger}\boldsymbol{d}_{\rm I} + (\boldsymbol{w}_{\rm J}^*)^{\dagger}\boldsymbol{w}_{\rm J}^* + \sigma_{\boldsymbol{e}}^2}$, where $\sigma_{\boldsymbol{e}}^2 = 2^{-B}(\boldsymbol{w}_{\rm J}^*)^{\dagger}\boldsymbol{w}_{\rm J}^*$.

Algorithm 1: Branch and Bound Based Beam Combination (BB-BC)

Input: Channel correlation matrix estimation $\boldsymbol{R}$; The number of combined beams K;
Output: The beam combination matrix, $\boldsymbol{A}_{\mathcal{C}}$;

Initialization: Set $\boldsymbol{R}_{\rm b} = \boldsymbol{R}$, $\boldsymbol{A}_{\mathcal{C}} = \phi$.
for *b=1:K* **do**
  Set $\mathcal{G} = \left\{\left(\boldsymbol{\Psi}^M, \phi\right)\right\}$. Set $\hat{\eta} = f(\bar{\boldsymbol{u}}_1, \boldsymbol{R})$, where $\bar{\boldsymbol{u}}_1$ is the dominant eigenvector of $\boldsymbol{R}_{\rm b}$ rounded to the nearest element in $\boldsymbol{\Psi}$ (entry-wise). Set $\boldsymbol{w}_b = \bar{\boldsymbol{u}}_1$.
  for $\mathcal{G} \neq \phi$ **do**
    Branch: Choose $\boldsymbol{S} \in \mathcal{G}$, which satisfies $\boldsymbol{S} = \arg\max_{\boldsymbol{X} \in \mathcal{G}} \eta(\boldsymbol{X}_2)$. Partition $\boldsymbol{S}$ into $\boldsymbol{S}_1$,..., $\boldsymbol{S}_{2^B}$, where $\boldsymbol{S}_i$ is the set satisfying $(\boldsymbol{S}_i)_2 = [(\boldsymbol{S})_2^T, \psi_i]^T$.
    Bound: Set $\mathcal{G} \leftarrow \mathcal{G} \backslash \boldsymbol{S}$. **for** $1 \leq i \leq 2^B$ **do**
      Calculate $\eta_i = f((\boldsymbol{S}_i)_2, \boldsymbol{R}_{\rm b})$, and $\boldsymbol{w}_i'$ is the corresponding optimum solution.
      if $\eta_i > \hat{\eta}$ **then**
        if $\mathcal{L}((\boldsymbol{S}_i)_2) = L$ **then**
          $\hat{\eta} = \eta_i$, $\boldsymbol{w}_b = (\boldsymbol{S}_i)_2$.
        else
          Set $\mathcal{G} \leftarrow \mathcal{G} \cup \boldsymbol{S}_i$
          Round $\boldsymbol{w}_i'$ to the nearest $\bar{\boldsymbol{w}}_i'$ in $\boldsymbol{\Psi}$.
          if $\eta(\bar{\boldsymbol{w}}_i') > \hat{\eta}$ **then**
            $\hat{\eta} = \eta(\bar{\boldsymbol{w}}_i')$, $\boldsymbol{w}_b = \bar{\boldsymbol{w}}_i'$
  Set $\boldsymbol{A}_{\mathcal{C}} \leftarrow [\boldsymbol{A}_{\mathcal{C}}, \boldsymbol{w}_b]$,
  $\boldsymbol{R}_{\rm b} \leftarrow \left(\boldsymbol{I}_L - \frac{1}{L}\boldsymbol{A}_{\mathcal{C}}\boldsymbol{A}_{\mathcal{C}}^H\right)^{\dagger}\boldsymbol{R}_{\rm b}\left(\boldsymbol{I}_L - \frac{1}{L}\boldsymbol{A}_{\mathcal{C}}\boldsymbol{A}_{\mathcal{C}}^H\right)$.
return $\boldsymbol{A}_{\mathcal{C}}$.

Proof: The proof is based on the rate-distortion theory. The details are omitted due to lack of space. ■

Based on Theorem 1 and Corollary 1, we are ready to develop the BB-based discrete beam combination (BB-BC) scheme. It is described in Algorithm 1. For $\boldsymbol{X} \in \mathcal{G}$, $\boldsymbol{X}_1$ and $\boldsymbol{X}_2$ denote the first and second entries of $\boldsymbol{X}$, respectively. ψ_i is the i-th entry of $\boldsymbol{\Psi}$. $f(\boldsymbol{d}, \boldsymbol{R})$ is defined as the optimum objective value of **P2** with CCM $\boldsymbol{R}$ and $\boldsymbol{d}_{\rm I} = \boldsymbol{d}$. The length of a vector $\boldsymbol{x}$ is denoted by $\mathcal{L}(\boldsymbol{x})$. $\eta(\boldsymbol{x})$ is defined in **P2**. The number of beams after beam selection is denoted by L.

The initial feasible solution is obtained by rounding the SVD-based solution to the nearest point in $\boldsymbol{\Phi}$, and the initial lower bound of the optimum is thus the objective function evaluated at this rounded point. The BB-BC works roughly as follows. We design beam combination weights for each column of the matrix $\boldsymbol{A}_{\mathcal{C}}$ successively and project to the orthogonal subspace of the CCM after selecting one column to avoid repetitive selection as in the 17-th step. It can be easily verified that $\left(\boldsymbol{I}_L - \frac{1}{L}\boldsymbol{A}_{\mathcal{C}}\boldsymbol{A}_{\mathcal{C}}^H\right)\boldsymbol{x} = 0$, $\forall \boldsymbol{x} \in {\rm range}(\boldsymbol{A}_{\mathcal{C}})$, where ${\rm range}(\boldsymbol{A}_{\mathcal{C}})$ denotes the column space of $\boldsymbol{A}_{\mathcal{C}}$. In each step, the BB-based scheme first branches on the existing candidate sets, each of which is possible to contain the optimum solution. The

branch criterion is to select one that is the mostly likely, based on the optimum objective function value $f(S_2, \boldsymbol{R})$ of each set $\boldsymbol{S}$ by Theorem 1. Compared with other branch criterion, e.g., width-first-search (branch the set with the smallest number of determined weights) or depth-first-search (branch the set with the largest number of determined weights), the adopted best-first approach shows better performance in terms of faster convergence in our simulations. After the branching, the branched sets are compared with the current best feasible solution by solving the continuous sub-problem for each set. The idea is that if the upper bound of the set is not as good as the current best feasible solution, it is unnecessary to keep branching that set. Therefore, the set is eliminated. Only the ones whose upper bound is better than the current best are retained as in the 12-th step. Meanwhile, we update the current best by rounding the optimum solution of the sub-problem if it is better. The algorithm continues until there is no more set to be branched.

It can be observed that the BB-BC searches over all the possible sets, and therefore is guaranteed to find the optimum solution. To accelerate the algorithm, one can adopt an alternative stopping criterion which ensures that the obtained maximum is near the optimum. The criterion can be written as $f(\boldsymbol{S}_2, \boldsymbol{R}_\mathrm{b}) - \hat{\eta} < \epsilon\hat{\eta}, \forall \boldsymbol{S} \in \mathcal{G}$. Then $\hat{\eta} > \frac{1}{1+\epsilon} \max_{\boldsymbol{S}\in\mathcal{G}} f(\boldsymbol{S}_2, \boldsymbol{R}_\mathrm{b}) > \frac{1}{1+\epsilon}\eta^*$. Hence the termination criterion ensures the resultant feasible solution is within $1/(1+\epsilon)$ of the optimum. Moreover, the Corollary 1 can be used to obtain an approximation of the upper bound $\hat{\eta}$ to further accelerate the convergence.

One can immediately come up with a sequential greedy beam combination (SG-BC) scheme which selects the best weights one by one based on Theorem 1. This heuristic scheme is also evaluated in the simulations.

V. Simulation Results

In this section, to test our proposed compression schemes, we will present simulation results using a link-level simulator based on the LTE numerology and 3GPP spatial channel models (SCMs). The spatial compression efficiency in (8) is adopted to evaluate the performance. Note that based on (8), we do not distinguish between useful signal and interference but focus purely on the retained signal power after spatial compression, due to the fact that the proposed spatial compression module is implemented in the RF and hence assumed to have no knowledge of the interference statistics. The spatial compression module takes time-domain signals as input and outputs the compressed dimensionality-reduced signal streams. The subsequent signal processing modules, such as orthogonal-frequqncy-division-multiplexing (OFDM) demodulation, decoding and etc., are exactly the same as the conventional LTE systems.

In Fig. 3, the comparison is made among the proposed schemes BB-BC and SG-BC, and the optimal combination scheme given by the SVD beamforming and beamspace transformation without beam combination. The baseline, i.e., performance without beam combination, is obtained by selecting

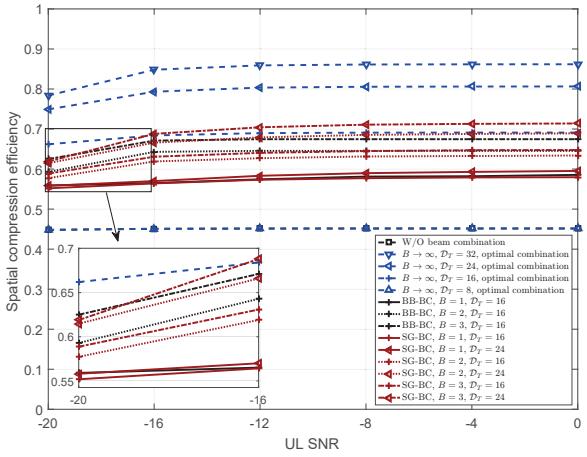

Fig. 3. Comparisons of proposed BB-BC, SG-BC, beamspace transformation without beam combination and optimal combination schemes with 128 antenna ports and 8 RF chains. The number of users is 2, and the user moving speed is 3 km/h.

a number of the strongest beams without beam combination. First, it is observed that beam combination after beamspace transformation is able to improve the spatial compression efficiency with the same number of RF chains. It is mainly due to spatial power leakage and imperfect channel statistics estimation which have been explained in Section III. Even with stringent hardware constraints, i.e., the resolution of digital phase shifters is limited and the amplitude is constant, the performance improvements over the one without beam combination is obvious, enabling us to adopt the proposed low-resolution PSN. It is seen that a one-bit PSN already improves the spatial compression efficiency by about 10%, and that a 2-bit PSN improves by 20%. Furthermore, a 3-bit PSN only has marginal performance advantage over 2-bit, meaning that a "dirty" low-resolution PSN is sufficient. On the other hand, the UL signal-to-noise-ratio (SNR) has little impact on the compression efficiency performance because the uplink CCM is estimated with a large number of OFDM symbols, which are from one LTE subframe and the whole bandwidth, i.e., $14 \times 1200 = 16800$ symbols. Note that the UL SNR is the per-antenna received SNR, and therefore the SNR of each beam after the beamspace transformation is much larger, e.g., M antenna elements bring about $10\log_{10} M$ dB beamforming gain. The other important note is that the performance of the SG-BC scheme is close to the optimal BB-BC scheme with hardware constraints. Given the dramatic complexity reduction by the SG-BC scheme (linear with the number of beams after beamspace transformation compared with exponential). It is much more desirable in practice.

A. Link-Level Simulations for Achievable Rates

In order to validate the proposed spatial compression performance in practice and also show that the compression efficiency metric is well related to real-system performance, a link-level LTE-based simulation is conducted. The spa-

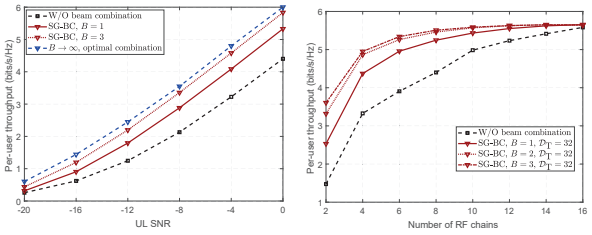

(a) (b)

Fig. 4. Link-level per-user throughput comparisons with 32 phase shifters and 8 RF chains. The number of users is 2 and the moving speed is 3 km/h.

tial compression is performed before the channel estimation module, which adopts a FFT-based scheme [17], and the baseband receiving algorithm to decode multi-user signals is MMSE-based. After the MMSE receiver, the decoded constellation points for the user are compared with the transmit ones to calculate the symbol-error-rate (SER). The simulator does not include channel coding and decoding to save processing time. The candidate modulation schemes are quadrature phase-shift keying (QPSK), 16-quadrature-amplitude-modulation (16-QAM) and 64-QAM. The SINR is mapped from the SER based on a predefined look-up table (with different modulation orders) and thereby the throughput is calculated based on the Shannon formula with the SINR derived before. The simulator only calculates the throughput of the first user for simplicity, and averaged over multiple drops. Therefore, the resulting throughput can be interpreted as per-user throughput. The link adaptation is enabled to support various SNRs whereby the BS estimates the SINR based on received sounding-reference-signals (SRSs) to decide the uplink transmit modulation-coding-scheme (MCS). No outer-loop link adaptation is used. All users are scheduled simultaneously (traffic type: full buffer) on the whole frequency bandwidth. The SRS which follows the 3GPP definition of Zadoff-Chu (ZC) sequences is enabled to simulate the LTE-based uplink traffic channel (PUSCH) transmissions. We run each drop for 200 ms, which corresponds to 20 radio frames in the LTE systems. Fig. 4(a) shows the comparison for a typical scenario, where the BS has 128 antenna ports, i.e., $2 \times 32 \times 2$ (rows $\times$ columns $\times$ polarizations), and the number of RF chains is 8. The number of beams after beamspace transformation is varied from 8 to 32. Similar performance trend as in Fig. 4(a) is observed, which shows that the proposed beam combination schemes can achieve higher throughput than the conventional beamspace MIMO system without beam combination given the same number of RF chains. In Fig. 4(b), the effect of RF chain reduction is presented by throughput simulation results. It is observed that considerable RF complexity reduction is possible by the proposed spatial compression schemes.

VI. Conclusions

In this paper, we propose to adopt a beam combination module after the beamspace transformation in beamspace MIMO systems to further reduce the RF complexity in beamspace MIMO systems. The fundamental reason that the RF chains can be saved by the proposed beam combination schemes is spatial power leakage by the lens antenna array and imperfect channel statistics estimations. The optimal beam combination with the hardware constrains is solved by the BB-BC scheme which is based on the BB methodology. The optimum solution to the sub-problem in the BB-BC is given in a closed-form which is key to the BB design. The spatial compression efficiency is used as the metric to compare proposed schemes and benchmarks based on a 3GPP SCM. It is observed that the proposed beam combination module can reduce the number of RF chains significantly (up to 25% with 1-bit PSN), and hence the RF complexity with low additional cost.

References

[1] R. W. Heath, N. Gonzlez-Prelcic, S. Rangan, W. Roh, and A. M. Sayeed, "An overview of signal processing techniques for millimeter wave MIMO systems," *IEEE J. Sel. Top. Signal Process.*, vol. 10, pp. 436–453, Apr. 2016.

[2] A. F. Molisch, V. V. Ratnam, S. Han, Z. Li, S. L. H. Nguyen, L. Li, and K. Haneda, "Hybrid beamforming for massive MIMO: A survey," *IEEE Commun. Mag.*, vol. 55, pp. 134–141, Sep 2017.

[3] Z. Jiang, A. Molisch, G. Caire, and Z. Niu, "Achievable rates of FDD massive MIMO systems with spatial channel correlation," *IEEE Trans. Wireless Commun.*, vol. 14, pp. 2868–2882, May 2015.

[4] Z. Jiang, S. Zhou, R. Deng, Z. Niu, and S. Cao, "Pilot-data superposition for beam-based FDD massive MIMO downlinks," *IEEE Commun. Letters*, vol. 21, pp. 1357–1360, Jun 2017.

[5] J. Brady, N. Behdad, and A. M. Sayeed, "Beamspace MIMO for millimeter-wave communications: System architecture, modeling, analysis, and measurements," *IEEE Trans. Ant. Propag.*, vol. 61, pp. 3814–3827, Jul 2013.

[6] P. V. Amadori and C. Masouros, "Low RF-complexity millimeter-wave beamspace-MIMO systems by beam selection," *IEEE Trans. Commun.*, vol. 63, pp. 2212–2223, Jun. 2015.

[7] Z. Jiang, S. Zhou, and Z. Niu, "Optimal discrete spatial compression for beamspace massive MIMO signals," *IEEE Trans. Signal Process.*, in press.

[8] A. Molisch, "A generic model for MIMO wireless propagation channels in macro- and microcells," *IEEE Trans. Signal Process.*, vol. 52, pp. 61–71, Jan. 2004.

[9] Y. Zeng and R. Zhang, "Millimeter wave MIMO with lens antenna array: A new path division multiplexing paradigm," *IEEE Trans. Commun.*, vol. 64, pp. 1557–1571, Apr. 2016.

[10] R. Schmidt, "Multiple emitter location and signal parameter estimation," *IEEE Trans. Ant. Propag.*, vol. 34, pp. 276–280, Mar 1986.

[11] Y.-C. Liang and F. P. S. Chin, "Downlink channel covariance matrix (DCCM) estimation and its applications in wireless DS-CDMA systems," *IEEE J. Select. Areas Commun.*, vol. 19, pp. 222–232, Feb 2001.

[12] X. Gao, L. Dai, S. Han, C. L. I, and X. Wang, "Reliable beamspace channel estimation for millimeter-wave massive MIMO systems with lens antenna array," *IEEE Trans. Wireless Commun.*, vol. 16, pp. 6010–6021, Sep 2017.

[13] A. Adhikary, J. Nam, J.-Y. Ahn, and G. Caire, "Joint spatial division and multiplexing: The large-scale array regime," *IEEE Trans. Inform. Theory*, vol. 59, pp. 6441–6463, Oct. 2013.

[14] S. Haghighatshoar and G. Caire, "Massive MIMO channel subspace estimation from low-dimensional projections," *IEEE Trans. Signal Process.*, vol. 65, pp. 303–318, Jan 2017.

[15] X. Gao, L. Dai, Z. Chen, Z. Wang, and Z. Zhang, "Near-optimal beam selection for beamspace mmwave massive MIMO systems," *IEEE Commun. Letters*, vol. 20, pp. 1054–1057, May 2016.

[16] A. H. Land and A. G. Doig, "An automatic method of solving discrete programming problems," *Econometrica: Journal of the Econometric Society*, pp. 497–520, 1960.

[17] P. Tan and N. C. Beaulieu, "A comparison of DCT-based OFDM and DFT-based OFDM in frequency offset and fading channels," *IEEE Trans. Commun.*, vol. 54, pp. 2113–2125, Nov 2006.